


 Cite this: *Nanoscale*, 2018, **10**, 19220

Stable-radicals increase the conductance and Seebeck coefficient of graphene nanoconstrictions†

 Mohammed Noori,^{a,b} Hatef Sadeghi  ^{*a} and Colin J. Lambert  ^a

Nanoscale thermoelectricity is an attractive target technology, because it can convert ambient heat into electricity for powering embedded devices in the internet of things. We demonstrate that the thermoelectric performance of graphene nanoconstrictions can be significantly enhanced by the presence of stable radical adsorbates, because radical molecules adsorbed on the graphene nanoconstrictions create singly-occupied orbitals in the vicinity of Fermi energy. This in turn leads to sharp features in their transmission functions close to Fermi energy, which increases the electrical conductance and Seebeck coefficient of the nanoconstrictions. This is a generic feature of radical adsorbates and can be employed in the design of new thermoelectric devices and materials.

 Received 15th June 2018,
 Accepted 2nd October 2018

DOI: 10.1039/c8nr04869j

rsc.li/nanoscale

Introduction

Graphene has attracted huge interest for its extraordinary thermal, mechanical, electrical and spintronic properties.^{1,2} It was recently demonstrated that stable electrode gaps below 5 nm can be formed using electroburning of graphene junctions.^{3–6} Motivated by recent experimental progress in using such electrodes to probe transport through single molecules,^{3,4,7–14} theoretical studies have also focused on the electrical properties of graphene nanoconstrictions formed by incomplete electroburning of narrow graphene junctions.^{3,14–18}

Graphene nanoribbons with zigzag edges have been predicted to show half metallic and spin filtering properties,^{19,20} with high densities of states near the graphene Fermi energy, which are attractive for thermoelectricity. However, these effects are not easy to isolate and control experimentally. In this paper, we demonstrate that states close to the graphene Fermi energy could be created by doping graphene constrictions with radical adsorbates, leading to a significant improvement in their electrical and thermoelectric properties. As prototypes for different non-radical and radical molecules, we dope the nanoconstriction with four different molecules (see Fig. 1) namely a non-radical pyridine (C_5H_5N) **1**, a pyridine

radical (C_5H_4N) **2**, a 4-picoline radical (C_6H_6N) **3**, and a methyl radical (CH_3) **4**.

Results and discussion

We investigate quantum transport through such constriction when each dopant **1–4** is attached to the narrow region of the constriction (shaded red dot Fig. 1a). In what follows, our aim is to investigate how the electrical and thermoelectric properties of graphene nanoconstrictions change when doping with one of these molecules. We calculate the transmission coefficient $T(E)$ which describes the probability that electrons with energy E can pass from the left to the right graphene electrode through the nanoconstriction (Fig. 1a). We first obtain

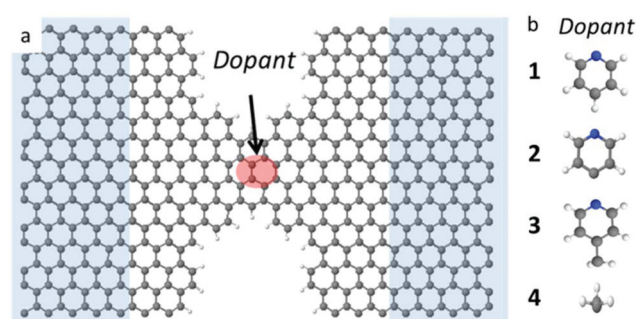


Fig. 1 (a) Schematic diagram of graphene nanoconstriction junction with four different dopants (b) graphene nanoconstriction junction with four different dopants **1** non-radical (pyridine), **2** pyridine radical, **3** 4-picoline radical, and **4** radical methyl group.

^aThe Theory of Molecular-scale Transport, Department of Physics, Lancaster University, Lancaster, UK. E-mail: h.sadeghi@lancaster.ac.uk, c.lambert@lancaster.ac.uk

^bDepartment of Physics, College of Science, University of Thi-Qar, Iraq

†Electronic supplementary information (ESI) available. See DOI: 10.1039/c8nr04869j



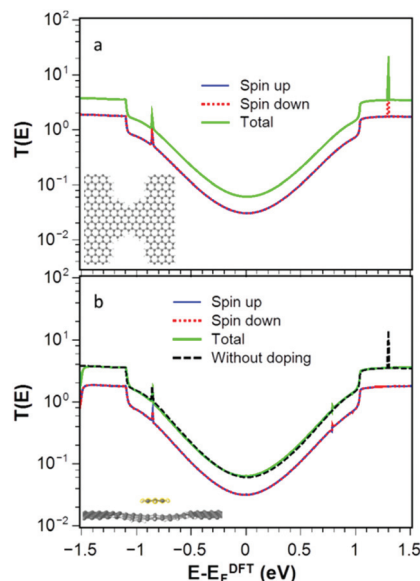


Fig. 2 The spin-dependent and total transmission coefficient as a function of energy for (a) a bare graphene nanoconstriction and (b) a graphene nanoconstriction junction with a non-radical adsorbate. The transmission coefficients for the spin up (blue line) and down (red dashed line) are identical.

the material-specific mean-field Hamiltonian of each structure from optimized geometry of each junction using the SIESTA implementation of density functional theory (see Method for detail). We then combine the DFT Hamiltonian with our quantum transport code Gollum to obtain $T(E)$ and use the Landauer formula to obtain electrical conductance G (see Methods for more detail). Since the radicals normally have unfilled orbitals, they are spin polarized. We therefore calculate the transmission function T_{\uparrow} for majority and T_{\downarrow} for minority spins. The total transmission function is defined to be $T(E) = (T_{\uparrow} + T_{\downarrow})$. With this notation, in the low temperature limit, the Landauer formula simplifies to $G = (e^2/h)T(E_F)$.

We have designed the graphene nanoconstriction of Fig. 1a to ensure that the graphene constriction is not spin polarized. To explore the electrical properties of the bare junction shown in Fig. 1a, we computed the transmission coefficient without doping. Fig. 2a shows the spin up (blue line), the spin down (red dashed line), and total transmission coefficient (green line). The transmission functions are independent of spin, which confirms that the bare junction is not spin polarized. Fig. 2b shows the spin dependent and total transmission coefficient for graphene nanoconstriction junction in the presence of non-radical pyridine 1. The solid lines in the graph show the transmission coefficient for the spin up, down and total transmission coefficient. For comparison, the transmission coefficient for bare structure is also shown in the graph by black dashed line. The transmission through this nanoconstriction is also non-spin polarized and it is apparent that introducing a non-radical dopant does not have a significant effect on the transmission coefficients.

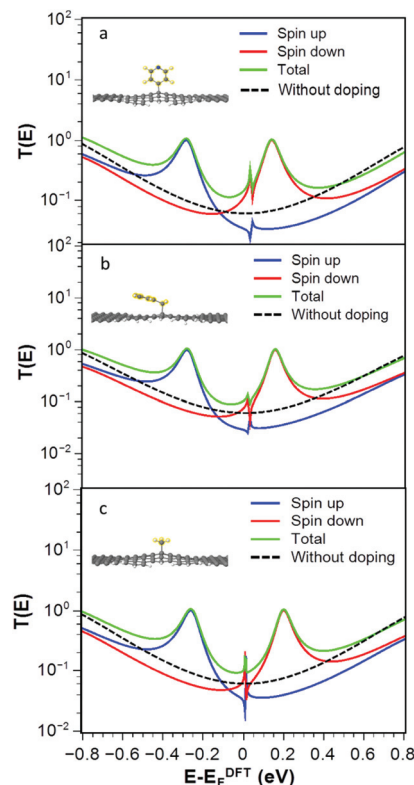


Fig. 3 The spin-dependent and total transmission coefficient as a function of energy for (a) pyridine radical nanoconstriction junction, (b) 4-picoline radical nanoconstriction junction, and (c) methyl group nanoconstriction junction.

For the radicals 2, 3 and 4, Fig. 3a–c show that the transmission functions become spin dependent. After geometry relaxation, we find that all three radicals are covalently bound to the graphene nanoconstrictions. As shown in Fig. 3, extra resonances close to the Fermi energy appear in the spin-dependent transmission coefficient. The total transmission coefficient (green curve) is much higher than the bare junction transmission (dashed black line) over a wide energy range near the Fermi energy. Regardless of the Fermi energy of leads, the conductance in the presence of the radicals is therefore predicted to increase. This is a general feature of these junctions and does not depend on the type of radical. This increase is due to the singly occupied orbital in the outer shell of the radical molecule.

Fig. 4a shows that the corresponding room-temperature electrical conductances with radicals (pyridine 2, 4-picoline 3 and methyl 4) are also much higher than those of the bare and non-radical cases. Fig. 4b shows that the presence of radical dopants not only enhances the electrical conductance of the graphene nanoconstrictions, but also it enhances the Seebeck coefficient of these junctions. Fig. 4b shows the Seebeck coefficients S of these junctions over a range of Fermi energies at room temperature. It is clear that large positive and negative values of S are achievable compared to bare and non-radical cases.

It is worth mentioning (see Fig. S1 and S2 of the ESI†) that doping of graphene nanoconstrictions with n-type and p-type



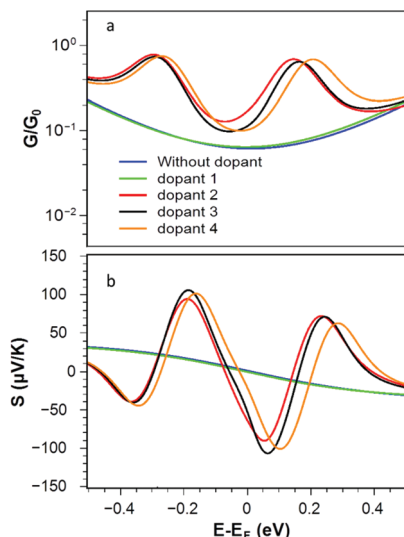


Fig. 4 (a) Electrical conductance and (b) Seebeck coefficient S for graphene nanoconstriction junction without dopant and with four different dopants: 1 non-radical (pyridine), 2 radical pyridine radical, 3 radical 4-picoline radical, and 4 radical methyl group.

dopants such as TTF and TCNE²¹ has a much less pronounced effect on the conductance and Seebeck coefficient of graphene nanoconstriction compared with stable radical adsorbates. TTF and TCNE create localised bound states, which are weakly coupled to the continuum of states in the graphene nanoconstriction, resulting in Fano-resonances. This leads to some enhancement, but not as strong as stable radical adsorbates.²⁰

Conclusion

We demonstrated a simultaneous increase in the electrical conductance and Seebeck coefficient of graphene nanoconstrictions using stable radical adsorbates, which create transmission resonances close to the Fermi energy. This increases electrical conductance up to an order of magnitude and enhances the Seebeck coefficient for a wide range of Fermi energies. The Seebeck coefficient of bare graphene nanoconstrictions is low, because the transmission function is symmetric with respect to the Fermi energy and therefore, its slope near the Fermi energy is low. In contrast, adsorbed radical create new spin states near the Fermi energy, which increases the slope of the transmission function and enhances the Seebeck coefficient. We demonstrated that this behaviour is a generic feature of graphene nanoconstrictions in the presence of adsorbed radicals.

Methods

The molecular device we study in this work is illustrated schematically in Fig. 1. The geometry of each graphene nanoconstriction junctions was relaxed to a force tolerance of 20 meV Å⁻¹

using the SIESTA²² implementation of density functional theory (DFT), with a double- ζ polarized basis set (DZP) and generalized gradient functional approximation (GGA-PBE) for the exchange and correlation functionals, which is applicable to arbitrary geometries. A real-space grid was defined with an equivalent energy cutoff of 150 Ry.

To calculate thermoelectronic properties of the molecules in the junction, from the converged DFT calculation, the underlying mean-field Hamiltonian H was combined with our quantum transport code, Gollum^{23,24} to calculate the transmission coefficient $T(E)$ for electrons of energy E passing from the source to the drain. The electrical conductance $G(T) = e^2/h(L_0^\uparrow + L_0^\downarrow)$, and the Seebeck coefficient²⁵ $S(T) = -(L_1^\uparrow + L_1^\downarrow)/|e|T(L_0^\uparrow + L_0^\downarrow)$, of the junction are calculated from the electron transmission coefficient $T(E)$ where $L_n^\sigma(T) = \int_{-\infty}^{\infty} dE (E - E_F)^n T_\sigma(E) \left(-\frac{\partial f(E, T)}{\partial E} \right)$ and σ is spin-up or down, $f(E, T)$ is the Fermi-Dirac probability distribution function $f(E, T) = (e^{(E-E_F)/k_B T} + 1)^{-1}$, T is the temperature, E_F is the Fermi energy, e is electron charge, and h is the Planck's constant.

Conflicts of interest

There are no conflicts to declare.

Acknowledgements

H.S. acknowledges the Leverhulme Trust for Leverhulme Early Career Fellowship no. ECF-2017-186. This work is supported by UK EPSRC grants EP N017188/1, EP/M014452/1 and the Ministry of Higher Education and Scientific Research, University of Thi-Qar, Iraq.

Notes and references

- 1 A. H. C. Neto, F. Guinea, N. M. R. Peres, K. S. Novoselov and A. K. Geim, *Rev. Mod. Phys.*, 2007, **81**, 109–162.
- 2 A. K. Geim and K. S. Novoselov, *Nat. Mater.*, 2007, **6**, 183–191.
- 3 H. Sadeghi, J. A. Mol, C. Siong, G. A. D. Briggs, J. Warner, C. J. Lambert, C. Lau, A. Briggs, J. Warner and C. J. Lambert, *Proc. Natl. Acad. Sci. U. S. A.*, 2016, **112**, 2658–2663.
- 4 F. Prins, A. Barreiro, J. W. Ruitenbergh, J. S. Seldenthuis, N. Aliaga-Alcalde, L. M. K. Vandersypen and H. S. J. J. Van Der Zant, *Nano Lett.*, 2011, **11**, 4607–4611.
- 5 S. Leitherer, P. B. Coto, K. Ullmann, H. B. Weber and M. Thoss, *Nanoscale*, 2017, **9**, 7217–7226.
- 6 C. Nef, L. Pósa, P. Makk, W. Fu, A. Halbritter, C. Schönenberger and M. Calame, *Nanoscale*, 2014, **6**, 7249–7254.



- 7 C. Jia, A. Migliore, N. Xin, S. Huang, J. Wang, Q. Yang, S. Wang, H. Chen, D. Wang, B. Feng, Z. Liu, G. Zhang, D. H. Qu, H. Tian, M. A. Ratner, H. Q. Xu, A. Nitzan and X. Guo, *Science*, 2016, **352**, 1443–1445.
- 8 P. Gehring, H. Sadeghi, S. Sangtarash, C. S. Lau, J. Liu, A. Ardavan, J. H. Warner, C. J. Lambert, G. A. D. Briggs and J. A. Mol, *Nano Lett.*, 2016, **16**, 4210–4216.
- 9 H. Sadeghi, S. Sangtarash and C. J. Lambert, *Beilstein J. Nanotechnol.*, 2015, **6**, 1413–1420.
- 10 J. A. Mol, C. S. Lau, W. J. M. Lewis, H. Sadeghi, C. Roche, A. Cnossen, J. H. Warner, C. J. Lambert, H. L. Anderson and G. A. D. Briggs, *Nanoscale*, 2015, **7**, 13181–13185.
- 11 C. S. Lau, J. A. Mol, H. Sadeghi, J. A. Mol, S. Sangtarash and C. J. Lambert, *Nano Lett.*, 2015, **1**, 1–7.
- 12 E. Burzurí, J. O. Island, R. Díaz-Torres, A. Fursina, A. González-Campo, O. Roubeau, S. J. Teat, N. Aliaga-Alcalde, E. Ruiz and H. S. J. Van Der Zant, *ACS Nano*, 2016, **10**, 2521–2527.
- 13 S. Lumetti, A. Candini, C. Godfrin, F. Balestro, W. Wernsdorfer, S. Klyatskaya, M. Ruben and M. Affronte, *Dalton Trans.*, 2016, **45**, 16570–16574.
- 14 H. Sadeghi, S. Sangtarash and C. Lambert, *Nano Lett.*, 2017, **17**, 4611–4618.
- 15 C. M. Tan, Y. H. Zhou, C. Y. Chen, J. F. Yu and K. Q. Chen, *Org. Electron.*, 2016, **28**, 244–251.
- 16 C. Jia, B. Ma, N. Xin and X. Guo, *Acc. Chem. Res.*, 2015, **48**, 2565–2575.
- 17 H. Sadeghi, S. Sangtarash and C. Lambert, *Phys. E*, 2016, **82**, 12–15.
- 18 N. Algethami, H. Sadeghi, S. Sangtarash and C. J. Lambert, *Nano Lett.*, 2018, **18**, 4482–4486.
- 19 Y. W. Son, M. L. Cohen and S. G. Louie, *Nature*, 2006, **444**, 347–349.
- 20 K. Nakada, M. Fujita, G. Dresselhaus and M. S. Dresselhaus, *Phys. Rev. B: Condens. Matter Mater. Phys.*, 1996, **54**, 17954–17961.
- 21 A. Vezzoli, I. Grace, C. Brooke, K. Wang, C. J. Lambert, B. Xu, R. J. Nichols and S. J. Higgins, *Nanoscale*, 2015, **7**, 18949–18955.
- 22 J. M. Soler, E. Artacho, J. D. Gale, A. García, J. Junquera, P. Ordejón and D. Sánchez-Portal, *J. Phys.: Condens. Matter*, 2002, **14**, 2745–2779.
- 23 J. Ferrer, C. J. Lambert, V. M. García-Suárez, D. Z. Manrique, D. Visontai, L. Oroszlany, R. Rodríguez-Ferradás, I. Grace, S. W. D. Bailey, K. Gillemot, H. Sadeghi and L. A. Algharagholy, *New J. Phys.*, 2014, **16**, 093029.
- 24 H. Sadeghi, S. Sangtarash and C. J. Lambert, *Nano Lett.*, 2015, **15**, 7467–7472.
- 25 H. Sadeghi, *Nanotechnology*, 2018, **29**, 373001.

